FINAL REPORT

EXPERIMENTS TO VERIFY NONPARALLEL STABILITY THEORY

At

Virginia Polytechnic Institute and State University
Blacksburg, Virginia

NASA GRANT # NSG1-608

by

WILLIAM S. SARIC
Department of Mechanical and Aerospace Engineering
Arizona State University
Tempe, Arizona 85287-6106

December 19, 1988

The effects of normal mass injection and suction on boundary-layer stability and transition are studied on a flat plate. Titanium panels, in which 0.063-mm-diam holes were drilled on 0.635 mm centers, are inserted in the plate. Suction level and distribution are variable. Disturbances are introduced by means of a vibrating ribbon and measurements of both mean- and disturbance-flow velocities are made with a hot wire. Disturbance amplitudes are measured as a function of Reynolds number, frequency and suction characteristics, and are compared with the previous results obtained over a Dynapore surface. Transition measurements under natural and forced conditions are also made. The stabilizing effects of suction are documented. It is also shown that very high local flow rates through the suctions holes (which approach a hole Reynolds number of 300) do not destabilize the flow. On the other hand, weak blowing lowers the transition Reynolds number, but is found not to cause serious problems.

Nomenclature

$A(x)$ = disturbance amplitude function

C_f = wall skin-friction coefficient, = $(2\nu/U_\infty)du/dy$

C_p = pressure coefficient, = $(p-p_\infty)(1/2\rho U_\infty)$

D = hole diameter of perforated material

F = dimensionless frequency, = $2\pi\nu f/U_\infty \times 10^6$

f = dimensional frequency, Hz

$\max |u'|$ = maximum value of $|u'|$ at a chordwise location

p = static pressure

p_∞ = freestream static pressure

Q = volumetric flow rate

R = Reynolds number, = $U_\infty \delta_r/\nu = \sqrt{Re_x}$

R_{TR} = transition Reynolds number, = $U_\infty x_{TR}/\nu$

Re' = unit Reynolds number per meter, = U_∞/ν

Re_D = hole Reynolds number, = $v_0 D/\nu$

Re_x = x-Reynolds number, = $U_\infty x/\nu$

U_∞ = freestream velocity

u = boundary-layer velocity in the streamwise direction

u' = fluctuating velocity component in the streamwise direction

$|u'|$ = rms of u'

V_0 = average normal-to-the-wall velocity through a suction strip

v_0 = local normal-to-the-wall velocity through a suction hole

v' = fluctuating velocity component in the normal direction

x = streamwise coordinate

x_{TR} = streamwise location of transition

y = normal coordinate

δ_r = boundary layer reference length, = $\sqrt{\nu x/U_\infty}$

$\delta*$ = displacement thickness

η = boundary-layer variable in the direction normal to the wall, = y/δ

θ = momentum thickness

ν = kinematic viscosity

ρ = density

I.   Introduction

Since 1949 there has been much interest in increasing the range, endurance, and payload of long-range aircraft through the use of laminar flow control (LFC).[1-3] Overviews of the most current research in stability and transition and LFC are given in Refs. 4 and 5.   These efforts have been motivated by the realization that the skin friction of the turbulent boundary layer can account for up to 50% of the total drag on an aircraft during cruise.   Maintaining a laminar boundary layer by delaying transition to high Reynolds numbers substantially reduces the contribution to the overall drag and thus increases fuel efficiency.

It is well known that a laminar boundary layer is very difficult to maintain if special care is not taken, and the use of suction appears to be a promising approach to LFC. Because it is structurally impossible to manufacture a surface entirely of porous material, efforts have been made to discretize suction optimally by slots or strips.   Suction slots are expensive to fabricate and, because of the high mass flow rates associates with them, are subject to high Reynolds number instabilities such as separation and backflow.   These instabilities adversely affect the stability of the basic flow.

Recent attention has turned to strips of porous material. Dynapore, a woven stainless steel, first suggested by Pearce[6] and tested by Reynolds and Saric,[7] is less expensive to manufacture than slots and provides some structural support. The Dynapore surface is smooth enough to be acceptable for LFC, as shown by Reynolds and Saric[8] through detailed measurements that compared with the theory of Reed and Nayfeh.[9]   More recently, modern methods using electron-beam technology have been developed whereby very small, 63μm holes can be made with an electron beam in titanium.   The resulting perforated surface is very strong, with the potential of having surface quality (smoothness) superior to Dynapore.

The current work is motivated by three important questions that pertain to boundary-layer stability over porous surfaces. The first concerns the porous surface quality. Obviously, it is vital to have as smooth a surface as possible, to prevent additional disturbances from being introduced into the boundary layer.   Although Kong and Schetz[10] found a substantial increase in turbulent skin-friction drag over different porous surfaces, the concern for a laminar boundary layer is less serious than that for a turbulent boundary layer. It is also of interest to evaluate whether a porous titanium surface is superior to a woven stainless-steel Dynapore surface[8] for LFC use.   By duplicating the conditions in the earlier experiments of Reynolds and Saric[7,8] and by determining the disturbance amplitude curves, it is possible to compare results of the present titanium-panel experiments with the previous Dynapore-panel results and with the theory of Reed and Nayfeh.[9]

.

The second question motivating this work is oversuction. As the suction through a circular hole increases, vortical-like disturbances are created that may modulate unstable disturbance behavior. It is thought that, after a hole Reynolds number on the order of 10 is reached, the stability and transition characteristics of the boundary layer are influenced by the presence of the holes. Hence, the second objective of the experiment is to determine whether oversuction is a potential problem for LFC by measuring transition Reynolds number as the suction is increased. The roles of other dimensionless parameters in the problem are also determined and discussed.

The final question concerns the outflow caused by a strong pressure gradient across the suction plenum. Because of the low-pressure drop across the hole, when suction is applied near the leading edge of the airfoil strong pressure gradients may cause inflow in one region of the suction strip and outflow in the other region. The presence of outflow can possibly cause large destabilizing effects. It is the intention of this experiment to investigate the effect of relatively weak blowing on the transition Reynolds number. Moreover, it is necessary to determine whether or not there is any induced three-dimensionality caused by the blowing. In addition to the measurements, comparisons of displacement and momentum thicknesses and skin-friction coefficient with the calculated values from the two-dimensional theory are made.

II. Experimental Setup

A. Wind Tunnel Facility

The experiments were performed in the Virginia Polytechnic Institute and State University Stability Wind Tunnel. The facility is a closed-loop tunnel having a 9:1 contraction ratio to the test section, which is 1.83 m square and 7.31 m long, as shown in Figure 1. Seven turbulence-damping screens are located in the settling chamber, and these screens have an open-area ratio of 0.6. The flow is driven by a 4.3 m-diam fan that has eight constant-pitch blades. Turning vanes located in the settling chamber are spaced at 0.076-m intervals to help reduce any large-scale turbulence in the flow. The resulting flow in the test section is very uniform and steady, with a turbulence level of $|u'| = 0.02\%U_\infty$ at velocities up to 16 m/s.

Measurements are made exclusively with constant-temperature hot-wire anemometers. Data collection is handled through a data-acquisition system together with a spectrum analyzer. The system makes both dc and rms disturbance measurements serially from the various experimental instruments. Typically about 100 data points are taken and recorded during a single pass through a 7-mm thick boundary layer.

B. Flat-Plate Model

The experiments are conducted on a flat-plate model having a
1.83 m span, 3.66 m chord, and 0.021 m thickness. The model is a
laminated panel that consists of a 19 mm paper honeycomb core
sandwiched between two 1 mm 6061-T6 aluminum sheets. This design
is chosen for its light weight, strength, and very flat surface
that is insensitive to temperature and humidity changes. A
carefully contoured leading edge is used that has an elliptical
profile with a major-to-minor axis ratio of 67:1. Chordwise and
spanwise static pressure measurements are made by a total of 77
static pressure ports embedded in the surface of the plate along
one chordwise and two spanwise arrays. The diameter of the
pressure port is 0.41 mm. Differential pressures are measured
via scanivalves and a ±0.5 mm Hg differential-pressure
transducer. Except for the region near the leading edge, the
model has a zero pressure gradient to within $dC_p/dx < 0.0002$ cm^{-1}.

As shown in Figure 2, the flat plate is constructed to
accommodate four suction panels having 0.3 m chord and 0.91 m
span. In these experiments, perforated-surface panels are
located at positions 1 and 2, whereas solid-surface panels are
located at positions 3 and 4. The surface of the model is
carefully polished to reduce surface roughness, and special care
is taken at the leading-edge junction and around the panels to
provide flat, continuous surfaces. A variable-deflection
trailing-edge flap is attached to the downstream end of the flat
plate to control the position of the attachment line on the
leading edge. The flap is constructed from a 1.83 m x 0.28 m
plexiglass sheet hinged at the plate-flap junction and has a
tapered, sharp trailing edge.

In the absence of suction, transition to turbulence of the
laminar boundary layer on this model is found to occur aft of the
porous panels at $Re_x = 3.4$ x 10^6. Transition is defined as the
chordwise location where the sign of du/dx at fixed y changes
from negative to positive. The details are contained in Refs. 7
and 8.

C. Titanium Suction Panels

The skin of the porous suction panels is made of 0.6-mm-
thick titanium. Electron-beam drilled holes, 0.063 mm diameter,
on 0.635 mm centers at a sweep angle of 30 deg are distributed on
the skin. Since the holes are not lined up one after the other
in the stream direction, the influence and effect of any
upstream-hole disturbances are avoided. The titanium surface is
ideal for laminar flow control because of its rigidity and
extreme smoothness.

A schematic of the porous panels as installed in the model
is shown in Figure 3. The titanium is epoxied to a corrugated
paper sheet with the backing layer being a 3 mm fiberglass sheet.

The spanwise flutes in the corrugated sheet create suction strips
on the titanium surface, i.e., discrete sections of finite
streamwise extent (not to be confused with single rows of holes).
Because the flutes are sealed off from each other, suction can be
varied over any number of discrete 1.6 cm strips. The flute
arrangement is analogous to that of Reynolds and Saric,[8] except
that continuous-area suction is not possible.

The suction flow is provided by a 12.4 m^3 vacuum tank. The
total mass flow rate from the porous surfaces into the plenum
tank is held constant by a choked sonic nozzle. In this way, the
vacuum pumps and other sources of noise downstream are isolated
from the suction panels. The flow rate from each porous panel is
monitored by an in-line flow meter of the vortex-shedding type.
These have a flow range of 0.12 and 4.67 liters/s and a linearity
of 3% of full scale. The calculated mass flow rates through the
nozzle agree with those measured by the vortex flow meters, which
indicate that there are no leaks in the system.

D.   Vibrating Ribbon

Carefully controlled, constant-frequency disturbances are
introduced with a vibrating ribbon made of a phosphor-bronze
alloy located 120 cm from the leading edge of the plate. The
ribbon, 0.025 mm thick and 2.5 mm wide, is centered and stretched
0.4 m across the span; this is the freely vibrating length of the
ribbon. The tension in the ribbon is 20 N, a value found to
result in natural frequencies in the neighborhood of 180 Hz, well
above the range of frequencies used in these experiments. The
ribbon is isolated from the plate by two 0.2-mm-diam glass rods
outboard of which the ribbon is taped to the plate after being
insulated by a layer of transparent tape. Careful placement of
the ribbon in the boundary layer makes it possible to operate at
freestream velocities of U_∞ = 15-20 m/s without exciting a flow-
induced vibration of the ribbon. When placed in a constant
magnetic field, the ribbon then vibrates at the frequency of the
alternating current passed through it, and two-dimensional,
constant-frequency disturbances (the two-dimensional Tollmien-
Schlichting waves) are introduced into the boundary layer. For
further details, see Ref. 8.

III.   Procedures

Transition Reynolds number and disturbance-amplitude growth
are used as meaningful indicators of stability characteristics.
The two techniques are first used as a diagnostic to verify the
basic state (without suction, but with the panels intact) of a
flat-plate flow with zero pressure gradient and high transition
Reynolds number. The results obtained and presented in the next
section agree well with previous experiments[7] and linear
stability theory.

A.   Transition Measurements

Transition measurements are accomplished through the use of a fixed probe mounted on the plate. With the hot wire at constant physical height in the boundary layer, freestream velocity vs boundary-layer velocity is plotted, and the transition Reynolds number is determined to be where the gradient of the boundary-layer velocity du/dU_∞ increases sharply with a small increase in tunnel speed. An example of this is shown in Figure 4a. This method is compared directly with the technique of measuring the mean velocity at different chord positions at a fixed height from the plate and fixed freestream velocity. In this case, transition is defined as the chord location where the sign of the streamwise gradient of the boundary-layer velocity du/dx changes from negative to positive. An example of this is shown in Figure 4b. In each case, the fixed-probe measurement gives the same results as the fixed-velocity measurements.[8] The fixed-probe measurement is preferred because of its easy operation and because slight irregularities in the porous surface produce scatter in the data when the fixed-velocity technique is used. The measurements of Figure 4 are taken over a porous surface. The fixed-probe-type measurements of transition Reynolds number are used exclusively in this work in the oversuction and blowing tests.

B.   Disturbance-Amplitude Growth Measurements

One of the objectives of the experiment is to compare the titanium porous surface with the Dynapore panels (a woven stainless steel) used by Reynolds and Saric.[7] The basic boundary-layer stability experiment is used to verify the porous stability measurements. The vibrating ribbon creates fluctuating velocity components u' and v' in the chordwise and spanwise directions, respectively, superposed on the mean flat-plate boundary-layer flow. The distribution through the boundary layer of the rms disturbance velocity $|u'|$ is measured with the hot wire.

The growth of these disturbances (the two-dimensional Tollmien-Schlichting waves) is monitored at different chord positions downstream of the ribbon. Operating in the low-frequency range (approximately $F=20-25$, where F is the dimensionless frequency; $F = 2\pi v f/U_\infty \times 10^6$), the disturbance is first seen to decay in amplitude with Reynolds number, then experience growth and then decay if transition has not occurred in the unstable region. The Reynolds numbers R_I and R_{II}, where $d|u'|/dx = 0$, are known as the Branch I and Branch II neutral stability points, respectively. Between R_I and R_{II} the constant-frequency disturbance is unstable. The locus of points R_I and R_{II} as a function of dimensionless frequency F is the familiar neutral stability curve.

It is generally accepted that neutral stability measurements and measurements of minimum critical Reynolds numbers are not meaningful diagnostics for either transition or LFC. Rather, the total growth of disturbance amplitude (between R_I and R_{II}) is far more significant. This results in the so-called e^n methods proposed initially by Smith and Gamberoni[11] and Van Ingen.[12]

Several methods are possible for determining disturbance amplitude, $A(x)$ = $|u'|/U\infty$. For these experiments, the disturbance amplitude is determined through integration of the $|u'|$ profile across the boundary layer according to

$$A = \int_0^\infty \frac{|u'|}{U\infty} dy$$

This measurement is related in some sense to disturbance energy and minimizes scatter due to single-point measurements and nonparallel effects (see Ref. 13). Profile-shape changes due to suction are also included. The integration is carried out from the wall to the point of phase reversal, since, from mass balance consideration, this area must be one-half of the total area.

IV.   Results

A.   Stability Measurements

The present measurements show that titanium is an easier surface with which to work. The titanium surface is extremely smooth, resulting in a transition Reynolds number without suction of 2.4 x 10⁶ aft of the porous panels. This compares well with smooth-wall measurements made in this facility.[8] A comparison of the present measurements with the measurements of Reynolds and Saric[7] and the theory of Reed and Nayfeh[9] is shown in Figures 5 and 6.   Figure 5 illustrates the results of integrated disturbance amplitude vs R for a disturbance of frequency F=20 introduced into the boundary layer with one porous strip open on panel 1. The average suction velocity over the strip, V_0, is 5.5 x 10⁻³U∞, where U∞ = 14 m/s. The experimental results and the theory are in excellent agreement both with and without suction with less scatter over the titanium panels. Again, the suctionless results are included as a diagnostic to ensure that the presence of the holes is not disturbing the flow; i.e., the only factor affecting the basic state should be the suction. Figure 6 is for F=25, with seven strips open on panel 1 and three on panel 2. The total mass flow rate is the same as for the case of one porous strip, as described in Figure 5. This level is divided approximately in half for each of the two panels. The individual values of V_0 are 4.2 x 10⁻⁴U∞ and 1.1 x 10⁻³U∞, respectively. Again, the experiment and theory are in very good agreement. Moreover, the agreement with the previous experiments[7] is excellent. Because of this agreement, the suction optimization scheme predicted by Reed and Nayfeh[9] and demonstrated by Reynolds and Saric[7] is expected to hold in the

case of titanium panels. The theory,[9] a stability analysis of linearized of triple-deck, closed-form basic state, predicts that suction should be concentrated near the R_i position on the neutral stability curve for efficiency.

B.   Transition Measurements--Suction

The problem of oversuction is also of concern to those involved in LFC. The introduction of anything other than a flat surface can disturb a sensitive laminar boundary layer and possibly cause premature transition. In this case, the surface is a titanium panel with electron-beam-drilled perforations. The basic idea is that the flow through the circular holes will create streamwise vortices that would influence the stability and transition characteristics of the boundary layer. It has already been seen that at low suction levels the surface quality is such that the basic flow is unaffected by the presence of the holes. However, as suction levels are increased, the holes may cause nonuniformities, resulting in three-dimensionality and possible early transition. Since the span of a hot wire is about 1 mm, each hole is too small to be able to obtain the details of the three-dimensional disturbance, therefore, we must look at the integrated effect of all of the holes and choose transition Reynolds number as the best diagnostic. It is thought that one of the most important parameters is the "hole Reynolds number," $Re_p = v_0 D/v$, where v_0 is the local suction velocity through the hole and D is the diameter of the hole. It is believed that, above a certain level of Re_p, the holes introduce disturbances into the boundary layer, causing a destabilizing effect.

Figure 7 is a plot of transition Reynolds number as a function of hole Reynolds number. The results compiled in Figure 7 are for the case of one 1.6 cm strip open on panel 1 at x=195 cm from the leading edge. Because natural transition is too dependent on uncontrollable environmental conditions, "controlled" transition is induced with the vibrating ribbon. Here a disturbance of dimensionless frequency F=20 is introduced and transition forced at x=280 cm with Re_x = 2.4 x 10^6 for suctionless conditions. Since the transition measurements are made with different freestream velocities, the dimensional frequency f is changed in order to keep F constant. Moreover, the voltage to the vibrating ribbon is adjusted to keep the same level of $|u'|$ at the reference location of x=280 cm. Suction levels are varied and increased by changing chokes in the sonic nozzle. Three sizes are used--2.5 mm, 4.8 mm, and 6.8 mm diameter--resulting in very large volumetric flow rates of 1.05, 3.65, and 7.39 liters/s, respectively. In the case of the 7.39 liter/s flow rate, only the fully open condition and calculated mass flow rates are used. As shown in Figure 7, as suction levels through the single strip increase beyond practical limits with hole Reynolds numbers approaching 300, the transition Reynolds numbers are also found to increase. The curve flattens out at a transition Reynolds number of about 3.4 x 10^6, however,

this may be due more to naturally occurring disturbances tripping
the boundary layer, since this value is indeed the measured
natural transition of the flat plate.

C.   Transition Measurements--Mass Injection

When suction is applied near the leading edge of an airfoil,
strong pressure gradients over the finite chord of a suction
strip may cause inflow in the forward region of the strip and
outflow in the aft region. The presence of outflow can cause
large destabilizing effects as well as local three-
dimensionality. In Figure 7, transition Reynolds numbers are
shown for the cases of blowing through one strip and seven strips
open on panel 1. Both the one- and seven-strip cases are
included to show the effect of local blowing velocity on
stability characteristics; i.e., average mass flow rate is
constant, but the one-strip case has seven times the local
blowing velocity of the seven-strip case. Again, a disturbance
of dimensionless frequency, $F=20$, is introduced and transition
forced at $x=280$ cm with $Re_x = 2.4 \times 10^6$ for no-blowing
conditions. The 2.5-mm-diameter choke is used exclusively in the
sonic nozzle, and blowing levels are varied by the opening and
closing of a bleeder valve. Mass flow rates are monitored by
vortex-shedding flow meters linked to the spectrum analyzer. As
shown in the figure, no catastrophic effects on transition are
seen as blowing is increased, just a systematic reduction in
transition Reynolds number. To find the actual hole Reynolds
number Re_p and local blowing velocity $V_o/U\infty$ for the seven-strip
case from Figure 7, divide the valued given by 7.

In Table 1, comparisons of displacement thickness, momentum
thickness, and skin-friction coefficient with the two-dimensional
theory[9] are given. The boundary-layer mean-velocity profile u is
integrated numerically with displacement thickness $\delta*$ and
momentum thickness θ defined as

$$\delta* = \int_0^\infty \left(1 - \frac{u}{U\infty} \right) dy$$

$$\theta = \int_0^\infty \frac{u}{U\infty} \left(1 - \frac{u}{U\infty} \right) dy$$

In the process, the wall skin-friction coefficient C_f is found
pictorially by measuring the slope of the curve fit at the wall
according to

$$C_f = 2 \frac{v}{U\infty} \frac{du}{dy}$$

In the table, these quantities are compared with those obtained
from the two-dimensional theory of Reed and Nayfeh.[9] Here one
strip and seven strips are open on panel 1, and measurements are
taken at $x=220$ cm. The comparison is very good; however, it
cannot be inferred that no three-dimensionality exists. The

magnitude of the hole disturbance in comparison with the mean
flow is such that it is a lower-order quantity. Flow details
usually are not present in these integrated parameters. On the
other hand, it can be said that the flow is still laminar and the
hole disturbances have not caused transition. These results are
independent of whether one strip or seven strips is/are open on
the first panel. Since the one-strip case has seven times the
local blowing velocity of the seven-strip case, the insensitivity
to large blowing is shown.

V.   Conclusions

The stability experiments described in Sec. IV.A, besides
demonstrating that suction works, clearly show that the
effectiveness of suction is relatively independent of the type of
porous strip. Moreover, the two-dimensional stabiliy theory[9] can
accurately predict the behavior of Tollmien-Schlichting (T-S)
waves in the presence of discrete suction strips. This, in some
sense, obviates the need for additional two-dimensional
experiments of this type.

The transition measurements with suction described in Sec.
IV.B. show that large hole Reynolds numbers do not destabilize
the flow and oversuction may not be a problem if Re_p is the
important criterion. One can list other possible parameters for
hole suction, i.e.,
   1)   hole Reynolds number, $Re_p = v_0 D/v = 4Q/\pi Dv$
   2)   velocity ratio, $v_0/U\infty$
   3)   diameter/thickness ratio, D/δ_r (or $D/\delta*$, D/θ)
where v_0 is the local hole velocity. Other possibilities are a
Reynolds number ratio, Re_p/R, but this is just a combination of
parameters 2 and 3, or a hole Reynolds number based on freestream
velocity, i.e., $U\infty D/v$, but this is just a combination of
parameters 1 and 2. The x-Reynolds number has no meaning by
itself, but its effect must be combined (i.e., unit Reynolds
number) into one of the three parameters listed above. The only
possibility not included in the above group would be a Reynolds
number based on freestream velocity and a length scale
proportional to the local deflection of the streamlines due to
suction. This may be analogous to a roughness Reynolds number.
At this stage, not enough is known about this local streamline
deflection to be able to include it in the discussion. However,
one may conjecture that this is taken into account within the
three parameters listed.

In the present experiments, parameters 1 and 2, the hole
Reynolds number and the velocity ratio compare with the flight
situation. However, the diameter/thickness ratio is different by
a factor of 5. This is for flight Reynolds numbers of 20×10^6.
The importance of three-dimensionality of the disturbance will
occur on a scale of the order of a T-S wavelength. The
diameter/thickness ratio parameter is important in scaling the
relative size of the hole to the characteristic wavelength of the

T-S wave.   The   ratio of   hole diameter to the T-S wavelength is
2.5×10^{-3} in the   present experiments   and approximately 12×10^{-3} in
flight.   In both   cases this   ratio is   very small.   Therefore,
except for   the   caution   expressed   regarding   local   streamline
deflection Reynolds number, it would appear that one could extend
these results to flight conditions.

The transition   measurements with   blowing described in Sec.
IV.C. show   a systematic   reduction of transition Reynolds number
with mass   flow rate   that   is   independent   of   the   local   hole
velocity.   Moreover, while   blowing is destabilizing and reduces
the transition   Reynolds number,   its effects are not that severe
and probably   can be overcome by slightly increasing the suction.
In   fact, Pfenninger[14]   suggests that   one could   use weak blowing
near the   leading edge   to reduce   skin friction   and recover the
stability requirement with aft suction.

Acknowledgements

References

[1]Pfenninger,   W.,   "USAF   and   Navy-Sponsored   Northrop   LFC
Research Between   1949 and   1967," AGARD/VKI,   Special Course for
Drag Reduction, 1977.

[2]Hefner, J.N.   and Bushnell,   D.M.,   "An Overview of Concepts
for Aircraft   Drag Reduction,"   von Karman   Institute,   Rhode-St.
Genese, Belgium, March 1977, AGARD-R-654, p. 1.1.

[3]Bushnell, D.M.   and Tuttle, M.,   "Survey and Bibliography on
Attainment of Laminar Flow Control in Air Using Pressure Gradient
and Suction," Vol. 1, NASA RP-1035, 1979.

[4]*Viscous Flow   Drag Reduction*,   edited by   Gary Hough,   AIAA
Progress in   Astronautics and   Aeronautics, New   York,   Vol.   72,
1980.

[5]*Laminar-Turbulent Transition*,   edited by   R. Eppler   and H.
Fasel, IUTAM Symposium, Stuttgart, FRG, September 1979, Springer-
Verlag, New York, 1980.

[6]Pearce, W.E.,   "Application of   Porous Materials to Laminar
Flow Control," Paper 6693, Long Beach, California, 1978.

[7]Reynolds, G.A.   and   Saric,   W.S.,   "Experiments   on   the
Stability of the Flat-Plate Boundary Layer with Suction," *AIAA
Journal*, Vol. 24, Feb. 1986, pp. 202-207; (also AIAA Paper 82-
1026, 1982).

[8]Reynolds,. G.A. and Saric, W.S., "Boundary-Layer Suction
Experiments for Laminar Flow Control," VPI & SU Rept. VPI-E-
82.28.

[9]Reed,   H.L.   and   Nayfeh,   A.H.,   "Numerical-Perturbation
Technique for Stability of Flat-Plate Boundary Layers with
Suction," *AIAA Journal*, Vol. 24, Feb. 1986, pp. 208-214; (also
AIAA Paper 81-1280, 1981).

[10]Kong,   F.Y. and Schetz, J.A., "Turbulent Boundary Layer
over Porous Surfaces with Different Surface Geometries," AIAA
Paper 82-0030, 1982.

[11]Smith,   A.M.O. and   Gamberoni,   N.,   "Transition, Pressure
Gradient, and Stability Theory," Douglas Aircraft Co., Santa
Monica, California, Rept. No. ES 26388, 1956.

[12]Van Ingen, J.L., "A Suggested Semiempirical Method for the
Calculation of the Boundary-Layer Transition Region," Department
of Aeronautical Engineering, University of Technology, Delft, the
Netherlands, Repts. VTH-71 and -74, 1956.

[13]Saric, W.S. and Nayfeh, A.H., "Nonparallel Stability of
Boundary Layers with Pressure Gradients and Suction," AGARD CP
224, 1977.

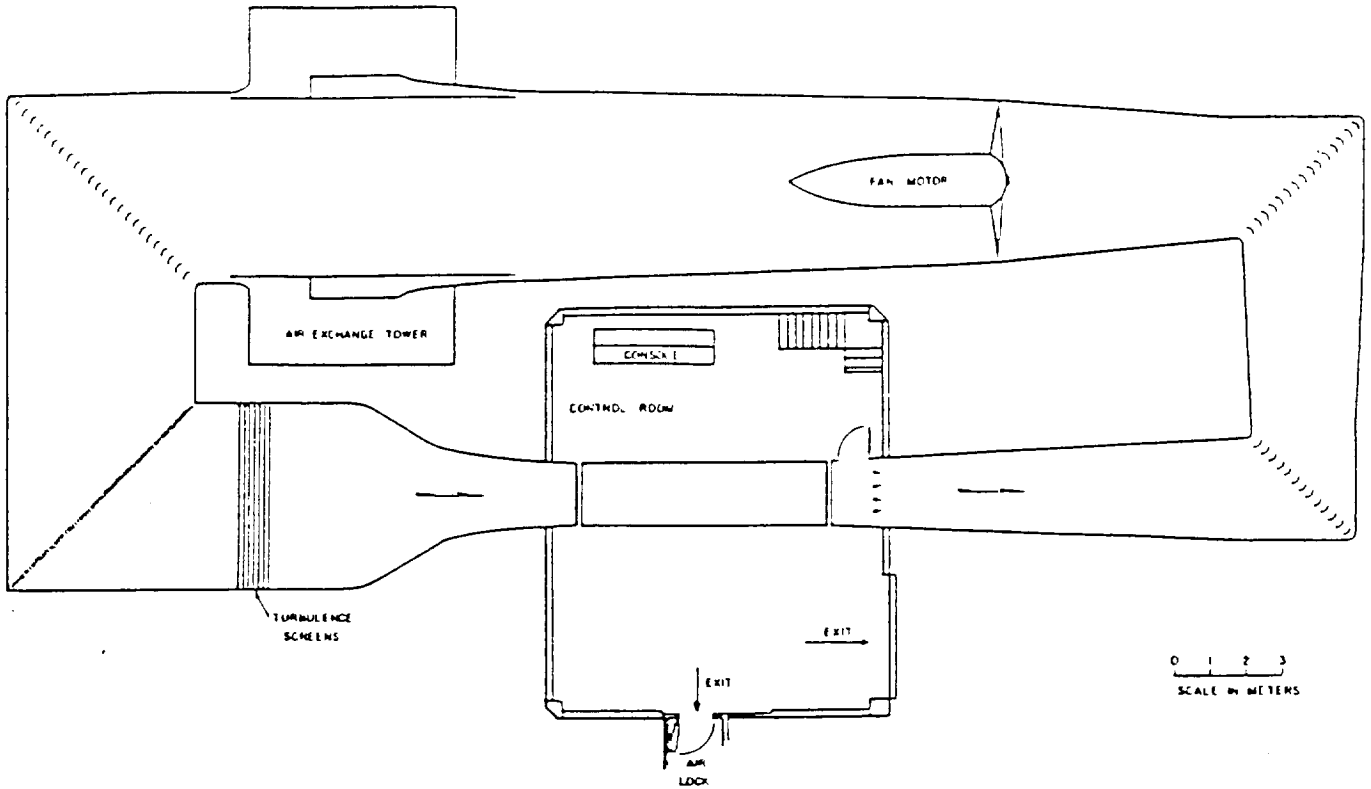[14]Pfenninger, W., Private communication.

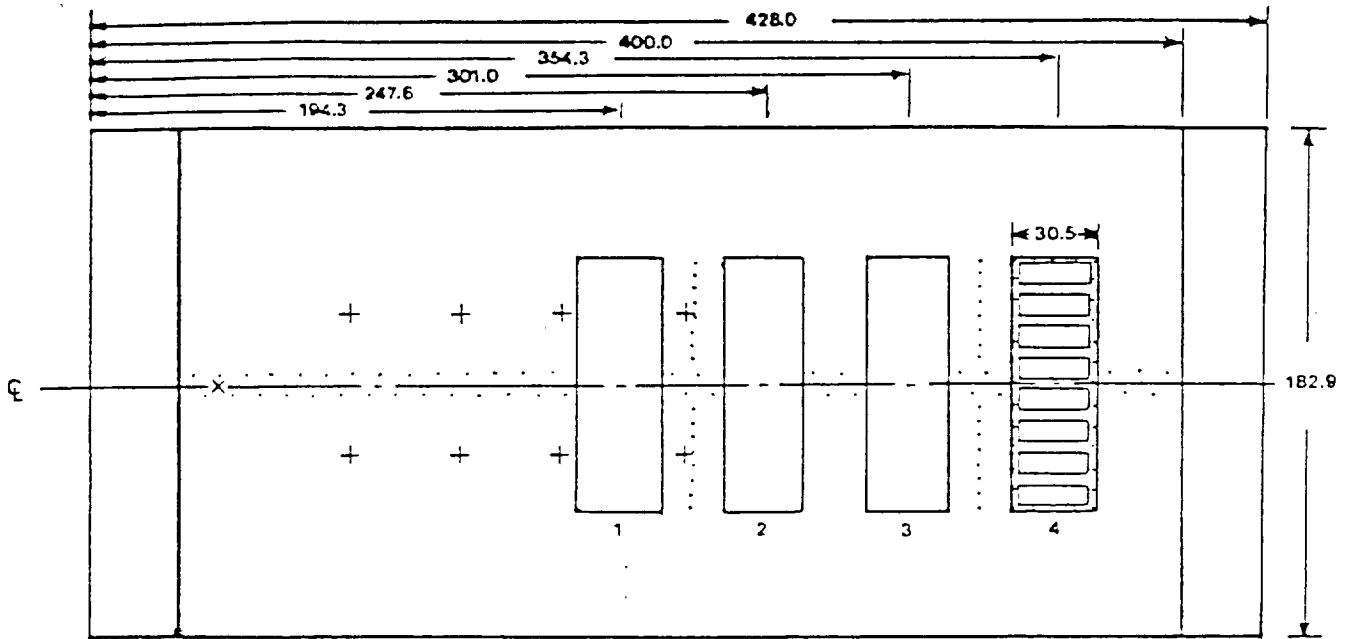Fig. 1 VPI & SU Stability Wind Tunnel, showing turning vanes, turbulence screens, control room, and test section.

Fig. 2 Flat-plate suction model, showing porous-panel locations as well as pressure ports •, inductance probe ◆, and smoke-wire locations ◆. Distances are in centimeters from the leading edge. The flap is indicated over the last 28 cm of the plate.
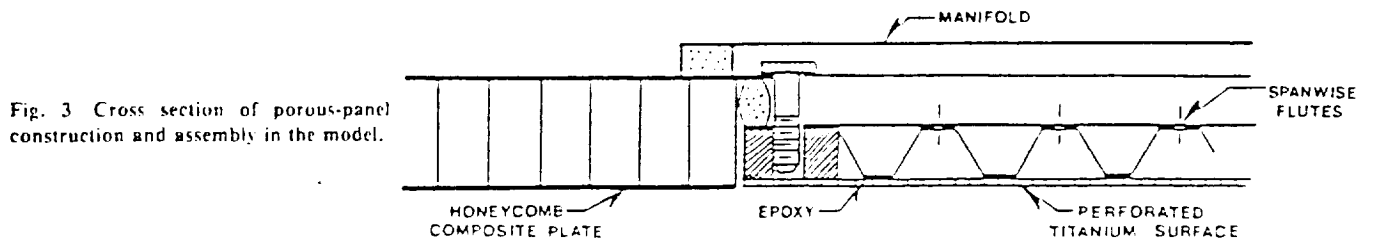

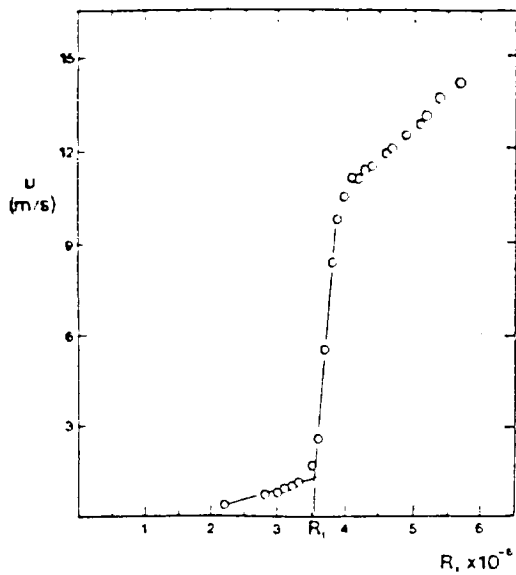Fig. 3 Cross section of porous-panel construction and assembly in the model.

Fig. 4 a) Transition Reynolds number obtained with the fixed hot-wire probe. $R_{TR} = 3.5 \times 10^6$.
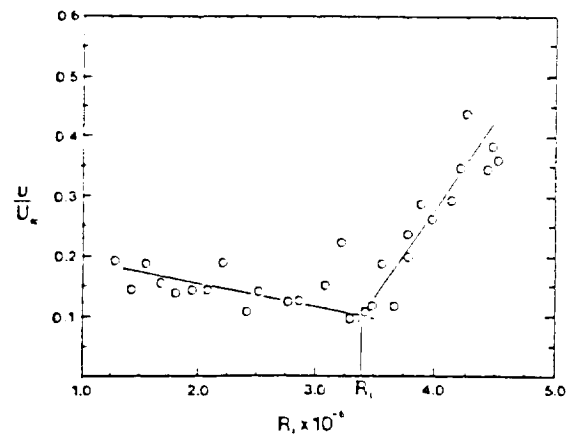

Fig. 4 b) Transition Reynolds number obtained with moving the hot-wire probe. $R_{TR} = 3.4 \times 10^6$. Strip locations and suction rates are indicated on the horizontal scale.
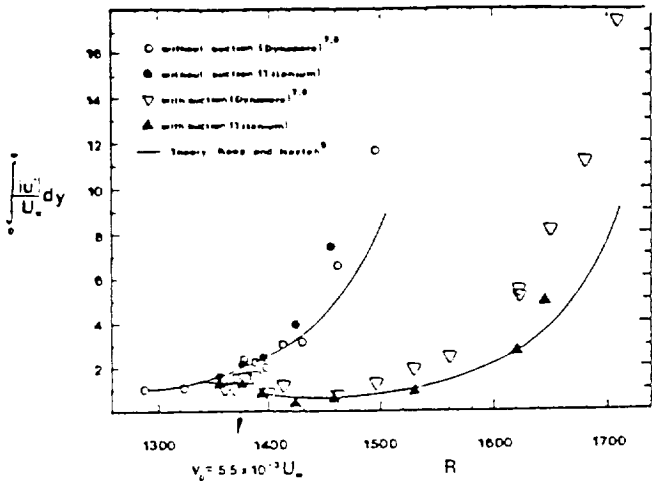

Fig. 5 Integrated disturbance amplitude vs Reynolds number. $Re' = 9.74 \times 10^5$, $U'_\infty = 14$ m/s, and $F = 20$. Strip locations and suction rates are indicated on the horizontal scale.
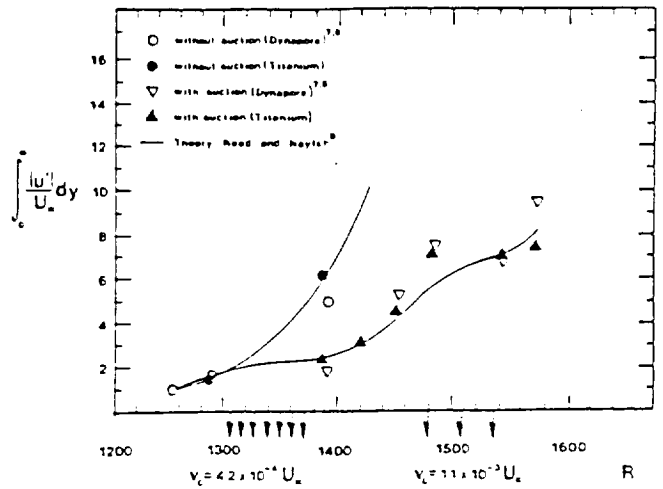

Fig. 6 Integrated disturbance amplitude vs Reynolds number. $Re' = 9.24 \times 10^5$, $U'_\infty = 14$ m/s, and $F = 25$. Strip locations and suction rates are indicated on the horizontal scale.
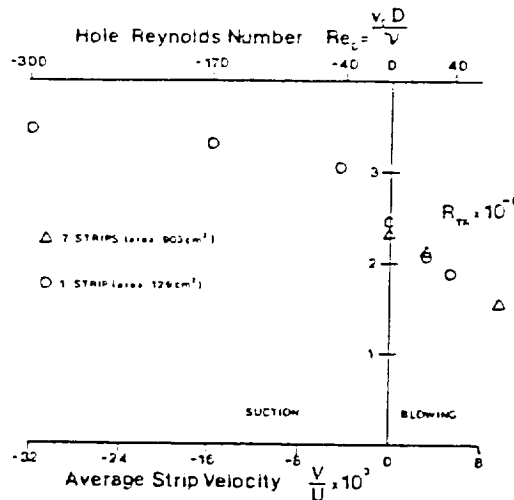

Fig. 7 Transition Reynolds number vs average strip velocity and hole Reynolds number. Results are for one 1.6 cm strip open at $x = 195$ cm. Transition is forced at $x = 280$ cm with $Re_s = 2.4 \times 10^6$ for suctionless/no-blowing conditions and $F = 20$. Note: To find the value of $V_c/U_\infty \times 10^3$ and Re_h for seven strips, divide the two values given by 7.

Table 1   Comparison of δ^*, θ, and C_f (experiment/theory) measurements taken at $x = 220$ cm

	Experiment	Theory
One strip, $Re' = 1.047 \times 10^6$ m^{-1}		
No blowing		
δ^*, mm	2.42	2.50
θ, mm	0.95	0.96
$C_f \times 10^3$	0.48	0.44
Blowing, $V_0/U_\infty = 0.00171$		
δ^*, mm	2.54	2.58
θ, mm	1.00	0.98
$C_f \times 10^3$	0.44	0.41
Seven strips, $Re' = 9.74 \times 10^5$ m^{-1}		
No blowing		
δ^*, mm	2.50	2.59
θ, mm	0.99	1.00
$C_f \times 10^3$	0.51	0.45
Blowing, $V_0/U_\infty = 0.00025$		
δ^*, mm	2.54	2.68
θ, mm	1.00	1.01
$C_f \times 10^3$	0.48	0.42
Blowing, $V_0/U_\infty = 0.00085$		
δ^*, mm	2.87	2.89
θ, mm	1.07	1.04
$C_f \times 10^3$	0.41	0.35